Environmental Science
Processes & Impacts

Accepted Manuscript

ROYAL SOCIETY OF CHEMISTRY

rsc.li/process-impacts

Quantitative measurement of nanoparticle size and number concentration from liquid suspensions by atomic force microscopy

M. Baalousha[§†+]*, *A Prasad*[†+] *and J. R. Lead*[§†]

[§] Center for Environmental Nanoscience and Risk, Department of Environmental Health Sciences, Arnold School of Public Health, University South Carolina, Columbia, South Carolina 29208

[†] School of Geography, Earth and Environmental Sciences, College of Life and Environmental Sciences, University of Birmingham, Edgbaston, Birmingham, B15 2TT, United Kingdom

[+] joint first authors

Corresponding author:* mbaalous@mailbox.sc.edu.

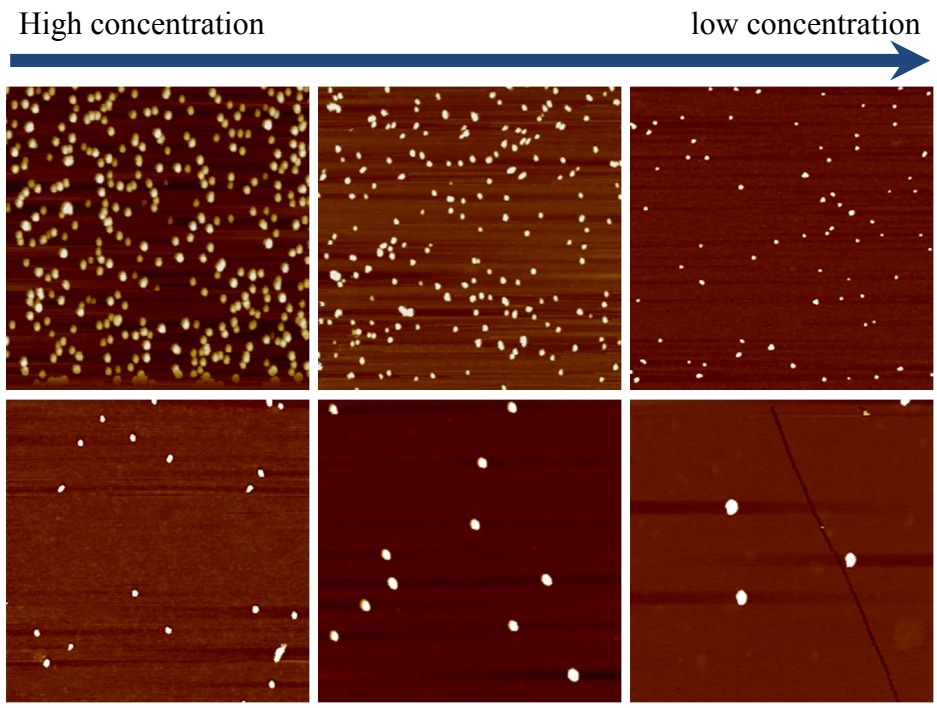

Table of Content (TOC) Art

Highlight: Validated fully quantitative approach to measure nanoparticle number concentration and number size distribution

Environmental Impact

The work presented here presents, for the first time, a fully quantitative sample preparation method for the measurement of number concentration and number size distribution of nanomaterials from dilute aqueous suspension (*e.g.* ppt-ppb range) using atomic force microscopy. The method presented here enhances the capabilities of atomic force microscopy for several applications in environmental nanoscience such as (i) measuring the number concentration dose in nanotoxicological studies and (ii) accurately measure the number size distribution of NPs, both are essential to understand the dose-response relationship for nanomaterials and are key requirement for the implementation of the European Commission recommendation for definition of nanomaterials.

Abstract

Microscopy techniques are indispensable in the nanoanalytics toolbox and can provide accurate information on nanoparticle (NP) number size distribution and number particle concentration at low concentrations (*ca.* ppt to ppb range) and small sizes (*ca.* <20 nm). However, the high capabilities of microscopy techniques are limited by the traditional sample preparation based on drying a small volume of suspension of NPs on a microscopy substrate. This method is limited by low recovery of NPs (*ca.* <10%), formation of aggregates during the drying process, and thus, the complete misrepresentation of the NP suspensions under consideration.

This paper presents a validated quantitative sampling technique for atomic force microscopy (AFM) that overcomes the abovementioned shortcomings and allows full recovery and representativeness of the NPs under consideration by forcing the NPs into the substrate via ultracentrifugation and strongly attaches the NPs to the substrate by surface functionalization of the substrate or by adding cations to the NP suspension. The high efficiency of the analysis is demonstrated by the uniformity of the NP distribution on the substrate (that is low variability between the number of NPs counted on different images on different areas of the substrate), the high recovery of the NPs up to 71%) and the good correlation (R>0.95) between the mass and number concentrations.

Therefore, for the first, we developed a validated quantitative sampling technique that enables the use of the full capabilities of microscopy tools to quantitatively and

accurately determine the number size distribution and number concentration of NPs at environmentally relevant low concentrations (*i.e.* 0.34-100 ppb). This approach is of high environmental relevance and can be applied widely in environmental nanoscience and nanotoxicology for (i) measuring the number concentration dose in nanotoxicological studies, and (iii) accurately measure the number size distribution of NPs, both are key requirement for the implementation of the European Commission recommendation definition of nanomaterials.

Introduction

Nanotechnology is a rapidly growing industry, which is expected to play a leading role in shaping the future of manufacturing processes and consumer products.[1] The number of consumer products apparently containing nanomaterials (NMs) has grown rapidly in the last decade and continues to grow.[2] Many of the applications of these novel materials will bring considerable improvements in quality of life and nanotechnology is an important economic and social driver. However, NMs also give cause for concern in terms of environmental and human health[3;4], which necessities in depth understanding of the fundamental of nano(eco)toxicity. Among those, understanding the dose-response relationship is essential in nano(eco)toxicology, where accurate quantification of the dose using appropriate metrics is a fundamental requirement. The number particle concentration is an important (eco)toxicology dose metric along with others (e.g. mass and surface area)[5;6] that requires accurate quantification. Hence there is a need for validated analytical tools/methods capable of providing fully quantitative assessment of the number size distribution and number particle concentration at environmentally/toxicologically relevant concentrations.

Furthermore, the environmental health and safety concerns of NMs drive the need to regulate NMs to ensure environmental and human safety. The first step in implementing such regulations is to accurately measure the dimensions and concentration of NMs. Several recommendations for definitions of NMs are currently available and are undergoing further development by international organisations.[7-9] These recommendations state that NMs are materials in the nanoscale size range that is 1-100 nm. More specifically, the EU recommendation for definition of NMs states that

"*nanomaterials are a natural, incidental or manufactured material containing particles, in an unbound state or as an aggregate or as agglomerate and where, for 50 % or more of the particles in number size distribution, one or more external dimensions is in the size range 1 – 100 nm.*".[9] Clearly, the accurate determination of number size distribution and number particle concentration of NMs are key components of the EU recommendations for definition of NMs and for the implementation of any EU regulations on NMs dependent on these recommendations.[9;10] However, the analytical tools to accurately quantify the number concentration of NMs are not appropriately developed or validated. Nanoparticles are a subset of nanomaterials with all three dimensions within the 1-100 nm range [7].

Several analytical techniques can provide information on number particle size distribution and/or number particle concentration such as nanoparticle tracking analysis (NTA), single particle-inductively coupled plasma-mass spectroscopy (sp-ICP-MS) and microscopy techniques.[11-13] These techniques suffer inherent limitations either in term of accurate sizing of nanoparticles (NPs), accurate determination of number concentration, the lower size limit or the availability of a standard validated procedure for sample preparation and analysis.[10;13] Other analytical methods deliver other NP size distributions (*e.g.* intensity for dynamic light scattering (DLS) and mass/volume for field flow fractionation (FFF when coupled to UV-vis or ICP-MS)) that need to be mathematically converted to the required number-based size distribution[13;14]. This conversion requires an accurate knowledge of particle properties (*e.g.* refractive index and absorption) and is based on a number of assumptions (*e.g.* the NPs are spherical, non-permeable and non-aggregated) and is thus prone to errors, difficult or even impossible if the mass fraction of NPs is not sufficiently large.[13-15] Additionally, the validation of the mathematical conversions of mass or intensity size distributions obtained by experimental measurements to number size distributions has not been performed.

Microscopy techniques (*e.g.* atomic force microscope (AFM) and transmission electron microscope (TEM)) have the potential to provide accurate measurement of NP number concentration and number size distribution[13;16]. So far, obtaining precise size and number concentration of NPs by microscopy techniques (*e.g.* AFM and TEM) has been limited by the sample preparation rather than by the capability of microscopy techniques

to count and measure the size of NPs. Different preparation techniques have been employed in the literature to prepare samples for microscopy analysis (AFM and TEM) including adsorption, drop deposition and ultracentrifugation.[13] These widely adopted sample preparation methods for microscopy analysis suffer mainly from poor statistical power, requiring the counting of large number of NPs to compensate for (i) low and inconsistent recovery of NPs on the sample substrate (*ca.* <10%) and (ii) non-uniform distribution of NPs on the sample substrate. The adsorption method is a passive method and depends largely on the diffusion of NPs to the substrate as well as the interaction between the NPs and the sample substrate, and thus the medium physicochemical properties. Hence, the adsorption method interrogates the smallest fraction of NPs with higher diffusion and those NPs that bind strongly to the AFM substrate (usually freshly cleaved mica).[17] The drop deposition method is known to induce aggregation artifacts due to reasons such as locally-increased salt concentrations on drying.[17] The ultracentrifugation method is an active method that forces all NPs in the suspension onto the AFM substrate; however, losses of NPs may occur after centrifugation due to the release of NPs from the substrate or during the essential washing process if the NPs are not strongly attached to the AFM substrate. Without substantive washing, severe artifacts can occur, which may result in analysis artifacts and bias, and these artifacts are discussed elsewhere.[18]

The objective of this study is to present a fully quantitative sample preparation method for AFM analysis that overcomes the above mentioned limitations. This method is based on combining substrate functionalization and ultracentrifugation to ensure high and uniform recovery of NPs on the AFM substrate and quantitative determination of the number of NPs and their number size distribution. The quality of the sample preparation is evaluated by the recovery of the NPs on the AFM substrate, the uniformity of NPs distribution on the AFM substrate, and the correlation between the mass and number concentrations.

Materials and Methods

Synthesis and characterisation of AuNPs. Gold nanoparticles (AuNPs) were synthesised in-house and were used without any further purification, cleaning or filtration (for details on AuNPs synthesis, see SI and references therein[13;19;20]). Two separate gold nanoparticle samples were produced, either coated in citrate (cit-AuNPs) or PVP (PVP-AuNPs). The synthesized NPs and were used in this study to assess the feasibility of measuring NP number concentration using AFM. The synthesised NPs were characterised a multimethod approach. Particle height, equivalent circular diameter, z-average hydrodynamic diameter was measured, number average hydrodynamic diameter and plasmon resonance were measured were measured by AFM, TEM, DLS, NTA and Uv-vis spectroscopy, respectively, and data are presented in supporting information (Table S1). TEM analyses were performed using TECNAI F20 Field Emission gun (FEG) TEM and samples were prepared by ultracentrifugation of the NPs on TEM grids using the same parameters as for AFM sample preparation (see details below). The two NPs (cit-AuNPs and PVP-AuNPs) were selected to represent charge and sterically stabilised NPs, respectively.

The mass concentration of AuNPs in the stock solution was determined by ICP-MS (Agilent 7500cs instrument, Wokingham, UK). One ml of stock suspension of AuNPs was diluted into 5 ml ultrahigh purity water (UHPW, 18 MΩ cm^{-1}) and 1.25 ml of concentrated aqua regia to achieve 20% aqua regia (Sigma Aldrich, Dorset, UK) to solubilise the gold NPs. The solution was then diluted 10 times to achieve 2% aqua regia acid in the suspension, which is suitable for ICP-MS analysis. The samples were further diluted 100 times in 2% aqua regia before analysis to match the calibration range of the ICP-MS; that is 0-100 ppb. The initial concentration of Cit-AuNPs and PVP-AuNPs were 101.6±3.2 and 167.6±3.2 mg L^{-1}. The dissolved fraction of AuNPs was determined following ultrafiltration (stirred ultrafiltration cell, Millipore, UK) using 1 kDa regenerated cellulose membrane (Millipore, UK) and measured by ICP-MS. The percentage dissolved gold ions were generally < 1%.

Sample preparation for atomic force microscopy. The AFM samples were prepared by ultracentrifugation of a suspension of NPs (11.1 ml) at 150000 g for 60 minutes using a Beckman ultracentrifuge (L7-65 Ultrcentrifuge, Beckman Coulter Ltd,

High Wycombe, UK) with a swing out rotor SW40Ti on a freshly cleaved mica substrate. A teflon insert was placed at the bottom of the centrifuge tube to create a flat surface that supports the mica substrate. The applied ultracentrifugation force is sufficient to collect all AuNPs larger than 5.0 nm, assuming gold density of 19.3 g cm^{-3} (Equations are provided in SI section)[21]. Two independent replicates of six different concentrations of cit-AuNP and PVP-AuNPs in the range of 1-100 ppb (Table 1 and 2) were prepared for AFM analysis. Two methods were examined to enhance the retention, distribution and recovery of NP on the substrate that is (i) surface functionalization of the substrate with a positively charged poly-l-lysine polymer (Sigma Aldrich, Dorset, UK) and (ii) addition of $CaCl_2$ to the NP suspension before ultracentrifugation.

For substrate surface functionalization, the freshly cleaved mica substrates were immersed in 0.1% poly-l-lysine for 15 minutes followed by rinsing three consecutive times in UHPW to remove excess poly-l-lysine, after which the mica substrates were left to dry overnight under ambient air conditions in a covered Petri dish. Both cit-AuNPs and PVP-AuNP suspensions in UHPW were prepared on poly-l-lysine functionalized mica substrates. After ultracentrifugation, the mica substrates were washed thoroughly by immersing them three consecutive times in UHPW for 30 seconds each, then the mica substrates were left to dry under ambient air conditions before ultracentrifugation of the suspensions of NP.

For the addition of $CaCl_2$ to the NP suspension prior to ultracentrifugation, PVP-AuNP samples were prepared in 10 mM $CaCl_2$, whereas Cit-AuNPs were prepared in (100-300 μM $CaCl_2$) on a bare AFM substrate. The higher concentration of $CaCl_2$ used for PVP-AuNPs compared with cit-AuNPs is due to the higher colloidal stability of PVP-AuNPs suspension compared to cit-AuNPs.[20]

AFM analyses. All AFM analyses were performed using an XE-100 AFM (Park systems Corp., Suwon, Korea). The measurements were carried out in true non-contact mode using a Silicon cantilever with a typical spring constant of 42 N m^{-1} (PPP-NCHR, Park systems Corp., Suwon, Korea). All scans were performed at ambient conditions, which have been shown to produce accurate sizing, despite loss of most, but not all water.[18;22] Images were recorded in topography mode with a pixel size

resolution of 256 × 256 and a scan rate of 0.5-1.0 Hz. Three different areas on each substrate were investigated and 5-9 images were collected from each area as described in Figure S1, resulting in 15-27 images being investigated for each substrate. On average, the time for AFM analyses per sample was about 2 hours. The scanned area per image varied between 1 μm x 1 μm to 5 μm x 5 μm depending on the sample concentration and the number of NPs on each image to facilitate NP counting. Height measurements of NMs were made using the transect analysis using the XEI data processing and analysis software of the microscope (Park Systems Corp., Suwon, Korea). For each sample, a minimum of 200 height measurements were performed, which are sufficient to produce a representative particle size distribution.[13] The measured heights were then classified into intervals of 0.5 nm to construct particle size distribution histograms, which was fitted with a log-normal distribution function as described elsewhere[13].

Evaluation of the AFM sample preparation. Several criteria are used to assess the efficiency and accuracy of the AFM methodology developed in this study including: (i) uniformity of NP distribution on the AFM substrate by comparing the number of particles counted at different areas on the AFM substrate, (ii) the % recovery of NPs on the mica substrate compared to the concentration of NPs in suspension and (iii) the correlation of number concentration measured by AFM *vs.* mass concentration in suspension (linearity).

The uniformity of NP distribution on the AFM substrate was evaluated by calculating the coefficient of variation (CV) of the number of NPs per μm^2 on the different images (CV = σ/mean of number NPs per μm^2 on the different images, where σ is standard deviation of number NPs per μm^2 on the different images). Low CV values indicate uniform distribution of NPs on the AFM substrate.

The number of NPs on each image was counted manually ($N_{counted/image}$) and then used to calculate the number of NPs (NP L^{-1}) in suspension ($N_{suspension}$) using Eq.1

$$N_{suspension} = \frac{N_{counted/image}}{V_{image}} \quad \text{Eq.1}$$

Where V_{image} is the volume of suspension above the area corresponding to each AFM image (in litres), which can be calculated according to Eq.2

$$V_{image} = A_{image} h \quad \text{Eq.2}$$

Where A_{image} is the area of each image and h is the height of water column on top of the image and was calculated using Eq.3

$$h = \frac{V_{centrifuged}}{\pi r^2} \quad \text{Eq.3}$$

Where $V_{centrifuged}$ is the volume of centrifuged NP suspension (*i.e.* 11.1 ml) and r is the radius of the centrifuge tube (r=6.85 mm).

The mass of NPs ($M_{recovered}$) in suspension can be calculated from the number of NPs in suspension (calculated in Eq.1) according to Eq.4 (ignoring size polydispersity by using the average particle diameter) or Eq.5 (taking into account size polydispersity by using the average particle diameter)

$$M_{recovered} = N_{suspension} v \rho \quad \text{Eq.4}$$

Where v is the volume of the average NP and ρ is the density of the NPs

$$M_{recovered} = \sum_{d_0}^{d_f} N_i v_i \rho \quad \text{Eq.5}$$

Where N_i is the number of NPs in each size subcategory, v_i is the volume of NPs in each size subcategory and d_0 and d_f are the minimum and maximum particle diameter.

The total centrifuged mass of NPs ($M_{centrifuged}$) in the centrifuged volume ($V_{centrifuged}$) can be calculated according to Eq.6

$$M_{centrifuged} = C_{suspension} V_{centrifuged} \quad \text{Eq.6}$$

Where $C_{suspension}$ is the concentration of NPs in the centrifuged suspension. Equation 5 assumes that AuNPs are insoluble, which is confirmed by the dissolution analysis (data not shown here).

The recovery of NPs on the AFM substrate can be calculated according to Eq.7 assuming that the NPs are insoluble and spherical. Using the mass calculated in Eq.4 gives the recovery by ignoring polydispersity, whereas using the mass calculated in Eq. 5 takes into account size polydispersity

$$\%recovery = \frac{M_{recovered}}{M_{centrifuged}} 100\% \quad \text{Eq.7}$$

The following assumptions are embedded in the calculation of the recovery: (i) no losses of NPs to the containers during storage, dilution and ultracentrifugation and (ii) all counted NPs are single entities and no interactions occurred between the NPs.

To determine the minimum number of images required to obtain accurate and statistically representative particle number concentration of the entire suspension of NPs, we investigated the stability of the calculated mean number concentration and standard deviation of the mean (σ_{mean}) on subpopulations of the scanned images (n=2-27 images).[12;13]

$$\sigma_{mean} = \frac{\sigma}{\sqrt{n}} \quad \text{(Eq.8)}$$

Results and discussion

We have established in previous studies on sample preparation (*e.g.* drop deposition, adsorption and ultracentrifugation) for AFM analysis that ultracentrifugation is the most appropriate sample preparation method providing the most representative number particle size distribution and number average sizes without assessment of sample recovery or uniformity of NP distribution on the substrate, which may result in inaccurate number concentration and number size distribution.[13;16;17] Obtaining precise number particle concentration and number size distribution by AFM can only be achieved by an improved sample preparation method that results in a) the quantitative deposition of NPs on to the substrate and b) a strong attachment mechanism that retains the NPs on the substrate during the essential washing process. In this work, we have overcome these challenges by combining NP ultracentrifugation to force all NPs to the substrate combined with addition of Ca^{2+} (cationic bridging) or poly-l-lysing (positively charged polymer) to more strongly attach the NPs to the mica substrate.[18] Below we discuss the quality of the sample preparation in terms of (i) uniformity of NP distribution on the substrate, (ii) NP recovery, (iii) number *vs.* mass concentration correlation and (iv) the minimum number of images required to achieve accurate number particle concentration and number size distribution.

Distribution of NPs on the AFM substrate

Qualitatively, AFM images of cit-AuNPs suspended in UHPW (Figure S2) or in 100-300 μM $CaCl_2$ (Figure S3-5) and PVP-AuNPs suspended in UHPW (Figure S6-7) ultracentrifuged on bare AFM substrate and PVP-AuNPs in UHPW ultracentrifuged on poly-l-lysine functionalised mica substrate (with or without washing the mica substrate after ultracentrifugation, Figure S8) show a rather non-uniform distribution of the NPs on the AFM substrate. In some areas, no NPs were observed and in other areas high number of NPs and aggregates were observed. This suggests that the NPs were not attached strongly to the AFM substrate and detached from and re-deposited during substrate washing resulting in losses of NPs at some areas and concentration and aggregation of NPs at other areas on the AFM substrate. The uniformity of NPs distribution on the substrate is crucially important to avoid the bias in counting the number of NPs if an area of low/high number of NPs is imaged and used to calculate number particle concentration in the ultracentrifuged suspension.

However, AFM images of cit-AuNPs in UHPW ultrancetrifuged on poly-l-lysine functionalized substrate (Figure S9) and of PVP-AuNPs in 10 mM $CaCl_2$ ultracentrifuged on a bare AFM substrate (Figure S10 and Figure 1) show uniformly distributed NPs on the substrate, presumably due to the strong and immediate attachment of the NPs to the AFM substrate following ultracentrifugation, preventing further particle displacement/interaction once sorbed to the substrate. Additionally, sample overloading was observed at concentration >100 ppb for the NPs investigated in this study (Figure S6 and S10). This overloading depends on the size and the density of the NPs being investigated, because for a given concentration of NPs in suspension, the number of NPs increases with the decrease in NP density and size.

Quantitatively, the distribution of cit-AuNPs and PVP-AuNPs in UHPW ultracentrifuged on bare AFM substrate and PVP-AuNPs in UHPW ultracentrifuged on poly-l-lysine functionalised AFM substrate was non-uniform (CV > 0.2, Figures S2 and S7-8 and Table S2-3). For citrate coated NPs, the addition of 100-300 μM Ca^{2+} ions have resulted in a slightly improved distribution of NPs on the AFM substrate in some but not all sample preparations (Figure S3-5, CV in the range 0.06-0.93, Table S2). Higher concentrations of Ca^{2+} cations results in extensive aggregation for cit-AuNPs and therefore has not been investigated. The distribution of cit-AuNPs in UHPW

ultracentrifuged on functionalized AFM substrate became more uniform (Figure S9, CV < 0.2, Table S2), presumably due to the strong attachment of the NPs to the substrate due to the charge attraction between the negatively charged cit-AuNPs and the positively charged functionalized substrate[23].

For PVP-AuNPs, the addition of 10 mM Ca^{2+} ions resulted in uniform distribution of the NPs on the AFM substrate (Figure 1 and S10, CV < 0.2, Table S3). Addition of $CaCl_2$ is likely to result in a strong attachment of the PVP-AuNPs to the mica substrate, possibly due to the bridging by Ca^{2+} of the negatively charged mica surface and the partially negatively charged PVP coating.[24] Therefore, addition of divalent cations to sterically stabilized NPs combined with ultracentrifugation may be used to improve the uniformity of NP distribution on the AFM substrate.

Recovery of NPs

The recovery of NPs on the AFM substrate was assessed by (i) ignoring NP size polydispersity (*e.g.* using the mass calculated in Eq.3) and (ii) considering NP size polydispersity (*e.g.* using the mass calculated in Eq.4). Accounting for size polydispersity results in a higher recovery (~2-5%, Table 3), indicating the importance of accounting for NP polydispersity when considering the size distribution and calculation of NP mass from microscopy techniques.[24] The samples studied here have very low polydispersity (CV is about 0.16 and 0.18). Samples with higher polydispersity will result in larger uncertainties in the calculated recoveries. Thus, the discussion below takes into account NP polydispersity when calculating NP recovery.

For AuNP samples in UHPW ultracentrifuged on the bare AFM susbtrate, recovery was very poor and was in the range of 0 to 0.5% for citrate-AuNPs and 4 to 45% for PVP-AuNPs. For citrate coated NPs, the addition of 100-300 μM Ca^{2+} ions have resulted in an increased recovery (1-27%) compared to that in UHPW and higher number concentrations of NPs, but also resulted in formation of aggregates of NPs (Figure S3-5), due to surface charge neutralization[25]. The functionalization of the AFM substrate with poly-l-lysine resulted in higher recovery of cit-AuNPs (48-71%, Table 3), but did not improve the recovery of PVP-AuNPs (sporadically few NPs were detected, Figure S8). The higher recovery of cit-AuNPs on the poly-l-lysine functionalized AFM substrate is

likely to be due to the strength of the attraction between the NPs and the substrate. Cit-AuNPs has a higher negative charge (zeta potential = -43 mV) compared with PVP-AuNPs (zeta potential = -8.3 mV), and thus cit-AuNPs are likely to be more strongly attracted to the positively charged poly-l-lysine functionalized AFM substrate than PVP-AuNPs. The addition of 10 mM $CaCl_2$ to PVP-AuNPs followed by ultracentrifugation on bare mica substrate resulted in an increased recovery of the NPs (26-45%, Table 3) and about an order of magnitude higher number concentration compared to those prepared in UHPW. The addition of 10 mM $CaCl_2$ to PVP-AuNPs did not induce any aggregation as PVP sterically stabilize the NPs[20]. The lower recovery for PVP-AuNPs compared to the cit-AuNPs is due to the presence of aggregates of PVP-AuNPs (Figure 4), which were not accounted for in the recovery calculations. The number of the aggregates represents about 35% of the counted particles; however, it is impossible to estimate the number of NPs within the aggregates by AFM. Some of the aggregates contained of 2 to 3 NPs, but other larger aggregates contain unknown number of NPs (Figure 4). These results suggest that the surface functionalization with oppositely charged polymer of the AFM substrate is the method of choice for electrostatically stabilized NPs; whereas for sterically stabilized NPs, the addition of divalent cations (*e.g.* Ca^{2+}) to enhance NP-substrate interactions is the method of choice. Nonetheless, assessment of the recovery of the NPs needs to be performed for other types of NPs due to the differences in the nature of NP-surface interactions, and further development might be required for other NPs.

Correlation between mass and number concentrations

The number particle concentration was measured at a range of concentrations to investigate the validity of the sample preparation method for different NP concentrations and to assess the range of applicability of the sample preparation method.

As expected given the recovery data, it was not possible to assess the correlation between the NP mass and number concentrations for cit-AuNPs in UHPW or in 100 μM $CaCl_2$ ultracentrifuged on bare mica substrate as well as for PVP-AuNPs in UHPW when ultracentrifuged on bare mica surface or poly-l-lysine functionalised mica substrate due to absence of NPs on the mica substrate in several samples (Table S2 and S3). The correlation between mass and number concentrations is poor for cit-AuNPs suspended in

300 μM $CaCl_2$ ultracentrifuged on bare mica surface (Figure S11b, R^2=0.26). Good correlation (Figure S11a, R^2=1.00) was observed for cit-AuNPs suspended in 200 μM $CaCl_2$ and ultracentrifuged on bare mica substrate, however the recovery of the NPs was very low (11.7±8.6%). The poor correlation and the low recovery of NPs in the above mentioned samples is presumably due to the inconsistent losses of NPs at different concentrations due to the weak attachment of the NPs to the AFM substrate.

For Cit-AuNPs, the functionalization of the substrate with poly-l-lysine resulted in an improved correlation (R^2= 0.999, Figure 2a). Similarly, for PVP-AuNPs, the addition of 10 mM $CaCl_2$ and ultrancentrifugation on bare mica substrate resulted in better correlation (R^2= 0.992, Figure 2a) between number and mass concentrations. The number of NPs counted per μm^2 of the mica substrate for cit-AuNPs ultracentrifuged on poly-l-lysine functionalized mica and for PVP-AuNPs in 10 mM $CaCl_2$ ultracentrifuged on bare mica substrate also shows a good correlation with the mass concentration (Figure 2b and Table S2-3) and suggests that the sample preparation method is applicable within the NP concentration range of 0.34-100 ppb for the NPs investigated in this study. Lower NP concentrations will result in higher uncertainty and variability because of the low number of NPs present on the AFM substrate (Figures S9-10, Table S2-3), or will require collecting more images to count sufficient number of NPs, which is becoming available in commercial AFM via AFM automation. Thus, the lower concentration limit can potentially be reduced to few tens of ng L^{-1}. Thus, the method presented here will allow quantitative analysis of low concentrations (ng to μg L^{-1}) of NPs to be performed, which are more representative of likely exposure scenarios from the environment,[26] consumer goods and the workplace and allows more realistic toxicology experiments to be performed. Higher NP concentrations will result in overloading (NP-NP interaction, Figures S9-10) of the AFM substrate and therefore it becomes impossible to obtain true counts of the NPs and to calculate NP recovery on the AFM substrate. The NP concentration range of 0.34-100 ppb is applicable for AuNPs of approximately 12-13 nm in diameter. However, the range of NP concentrations will depend on the size and composition (density) of the NPs (see discussion above).

Number of images required for representative measurement of number concentration

The effect of number of images on the mean number concentration and standard deviation of the mean for cit-AuNPs in UHPW prepared by ultracentrifugation on a poly-l-lysine functionalized substrate is shown in Figure 3 and for PVP-AuNPs in 10 mM $CaCl_2$ prepared by ultracentrifugation on bare mica substrate is shown in Figure S12. The mean number particle concentration tends to a stable value for ≥ 20 scanned images. The standard deviation of the mean generally decreases with the increase in the number of images and reaches a stable value at about ≥20 images. Therefore, 20 images is the required minimum number of images to obtain mean number concentration and standard deviation (σ) representative of the entire population of NMs.

The mean number concentration and standard deviation of the mean for cit-AuNPs suspended in 300 μM $CaCl_2$ prepared by ultracentrifugation on a bare AFM substrate and for PVP-AuNPs suspended in UHPW (data not shown here) are shown in Figure S13. Neither the mean nor the standard deviation tends to a stable value for the number of images scanned for all samples. Therefore, it is impossible to obtain a representative number particle concentration from these samples.

Number particle size distribution

The number size distribution of the cit-AuNPs and PVP-AuNPs together with the fitted distribution functions are shown in Figure 5. The number average size of cit-AuNPs and PVP-AuNPs was found to be around 13.3±2.1 nm (with a range 6.5-21 nm) and 12.2±2.2 nm (with a range 6.5-17 nm), respectively. The coefficient of variation was about 0.16 and 0.18 for PVP-AuNPs and cit-AuNPs respectively, suggesting that the two suspensions of NPs have relatively low polydispersity.[24] The number average sizes measured by TEM were 15.0±3.3nm and 10.0±2.8 nm for cit- and PVP-AuNPs respectively, in good agreement with the particle heights measured by AFM (Table S1). The z-average hydrodynamic diameters for cit- and PVP-AuNPs were 21.4 and 20.6 nm, respectively. The larger sizes measured by DLS can be attributed to the weighting (intensity based for DLS) and the permeability of the NPs, in particular the PVP-AuNPs [13].

Conclusions

This paper presents, for the first time, a validated sample preparation method for AFM that enables the full quantitative analysis of NPs number concentrations and number size distribution by AFM at environmentally and toxicologically relevant concentrations (*i.e.* 0.34-100 ppb). This method is based on forcing the NPs onto a substrate via ultracentrifugation and the NPs strong attachment due to surface functionalization of the substrate or by adding cations to the NP suspension. The method was validated using well stabilized AuNPs (coated by PVP or citrate) using the following criteria (i) NP recovery on the substrate, (ii) distribution of NP on the substrate, (iii) correlation between mass and number concentrations. Both citrate- and PVP-AuNPs were uniformly distributed on the substrate; that is the coefficient of variation between the numbers of NPs counted on different areas of the substrate was < 0.20. The recovery of the NPs on the substrate was quantified for the first time and it was up to 71%. The number of counted NPs correlated well (R>0.95) with the concentrations of NPs in suspension.

Future research will investigate the applicability of this sample preparation method for TEM, which will enable overcoming some of the AFM limitations such as determining the number of NPs within the aggregates and distinguishing between natural and manufactured nanoparticles when coupled with spectroscopy techniques.

Acknowledgement

We acknowledge funding and support from the Natural Environmental Research Council (NERC, NE/F005008/1 and NE/G004048/1), the EU FP7 MARINA project (263215), the NERC funded Facility for Environmental Nanoscience Analysis and Characterization, and the Center for Environmental Nanoscience and Risk (CENR) at the University of South Carolina.

Supporting Information Available

The supporting information provides AFM images of all the studied samples.

Reference List

1. Global Industry Analysts Inc., http://www.prweb.com/releases/nanotechnology/nano_products/prweb4719764.htm , 2011.

2. Woodrow Wilson data base. The project on emerging nanotechnologies (http://www.nanotechproject.org/). 2012.
Ref Type: Internet Communication

3. J. Fabrega, S. N. Luoma, C. R. Tyler, T. S. Galloway, and J. R. Lead, *Environ.Int.*, 2011**, 37**, 517.

4. S. J. Klaine, P. J. J. Alvarez, G. E. Batley, T. F. Fernandes, R. D. Handy, D. Y. Lyon, S. Mahendra, M. J. McLaughlin, and J. L. Lead, *Environ.Toxicol.Chem.*, 2008**, 27**, 1825.

5. G. Oberdörster, E. Oberdörster, and J. Oberdörster, *Environ.Health.Perspec.*, 2005**, 113**, 823.

6. G. Oberdörster, E. Oberdorster, and J. Oberdorster, *Environ.Health.Perspec.*, 2007**, 115**, A290.

7. BSI, *Terminology for nanomaterials*, PAS 136:2007, BSI British Standards, 2007.

8. ASTM, *Standard Terminology*, ASTM E2456-06, 2012.

9. The European Comission, *Off.J.Europ.U.*, 2011**, 54**, L275/38.

10. T. Linsinger, G. Roebben, D. Gilliland, L. Calzolai, F. Rossi, N. Gibson, and C. Klein, *Requirements on measurements for the implementation of the European comission definition of the term nanomaterial*, EUR 25404 EN, European Commision. Joint Research Center. Institute for reference materials and measurements, Geel, Belgium, 2012.

11. D. M. Mitrano, A. Barber, A. Bednar, P. Westerhoff, C. P. Higgins, and J. F. Ranville, *J.Anal.Atom.Spectrom.*, 2012**, 27**, 1131.

12. R. D. Boyd, S. K. Pichaimuthu, and A. Cuenat, *Colloid Surf.A.Physicochem.Eng.Aspects.*, 2011**, 387**, 35.

13. M. Baalousha and J. R. Lead, *Environmental Science & Technology*, 2012**, 46**, 6134.

14. M. Baalousha and J. R. Lead, *Environmental Science & Technology*, 2007**, 41**, 1111.

15. M. Baalousha, F. v.d.Kammer, M. Motelica-Heino, and P. Coustumer, *Anal.Bioanal.Chem.*, 2005**, 308**, 549.

16. M. Baalousha, Y. Ju-Nam, P. A. Cole, B. Gaiser, T. F. Fernandes, J. A. Hriljac, M. A. Jepson, V. Stone, C. R. Tyler, and J. R. Lead, *Environ.Toxicol.Chem.*, 2012**, 31**, 983.

17. R. F. Domingos, M. Baalousha, Y. Ju-Nam, M. Reid, N. Tufenkji, J. R. Lead, G. G. Leppard, and K. J. Wilkinson, *Environmental Science & Technology*, 2009**, 43**, 7277.

18. M. Baalousha and J. R. Lead, *Colloid Surf.A: Physicochem.Eng.Asp.*, 2013**, 419**, 238.

19. I. Römer, T. A. White, M. Baalousha, K. Chipman, M. R. Viant, and J. R. Lead, *J.Chromatogr.A.*, 2011**, 1218**, 4226.

20. A. Hitchman, G. H. Sambrook Smith, Y. Ju-Nam, M. Sterling, and J. R. Lead, *Chemosphere*, 2013**, 90**, 410.

21. T. Svedberg and J. B. Nichols, *J.Am.Chem.Soc.*, 1923**, 45**, 2910.

22. E. Balnois and K. J. Wilkinson, *Colloids Surf.A: Physicochem.Eng.Aspects*, 2002**, 207**, 229.

23. L. G. Harris, S. Tosatti, M. Wieland, M. Textor, and R. G. Richards, *Biomaterials*, 2004**, 25**, 4135.

24. M. Baalousha and J. R. Lead, *Nature Nanotechnol.*, 2013**, 8**, 308.

25. M. Baalousha, Y. Nur, I. Römer, M. Tejamaya, and J. R. Lead, *Sci.Tot.Environ.*, 2013**, 454-455**, 119.

26. F. Gottschalk, T. Sonderer, R. W. Scholz, and B. Nowack, *Environmental Science & Technology*, 2009**, 43**, 9216.

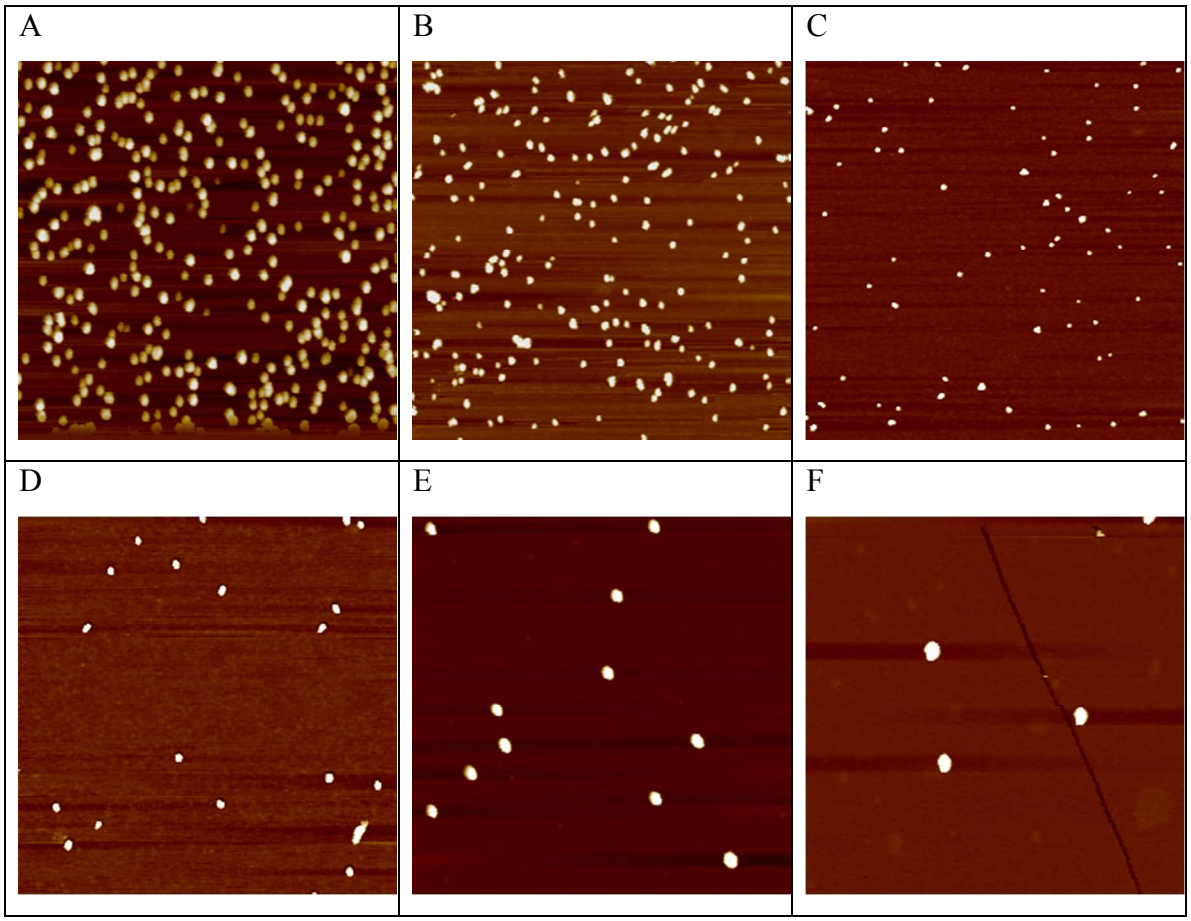

Figure 1. Representative atomic force microscopy images of PVP-AuNPs suspended in 10 mM $CaCl_2$ showing a uniform distribution of PVP-AuNPs on bare AFM substrate and the decrease of the number of NPs recovered with the decrease in NP mass concentration in ppb (a) 67.1, (b) 33.5, (c)16.8, (d)3.4, (e) 1.7 and (f) 0.34. All images are 2 µm x 2 µm.

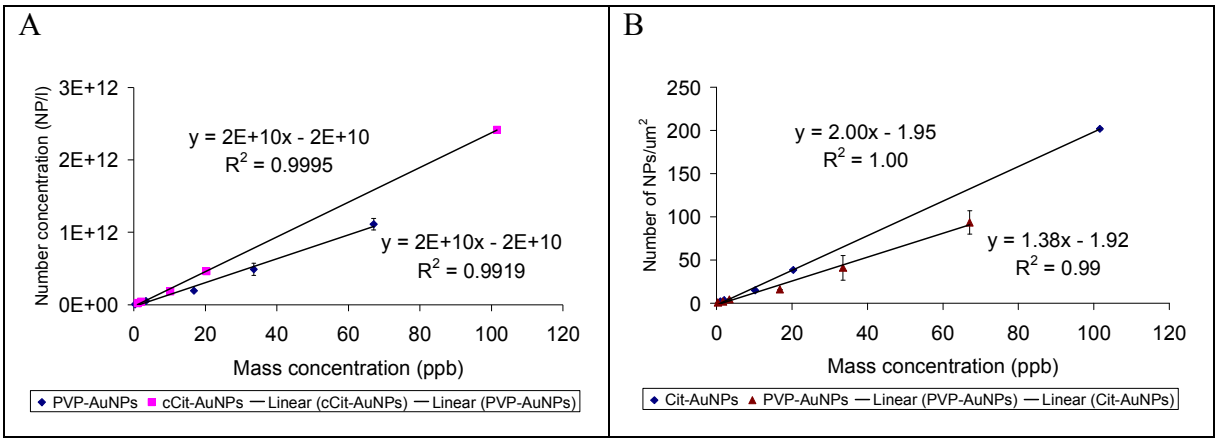

548 **Figure 2**. Correlation between the mass and number concentration of NPs (a) NP/l in
549 diluted suspension and (b) NP/μm^2 on the mica substrate. Cit-AuNPs was prepared by
550 ultracentrifugation on a poly-l-lysine functionalized mica substrate and PVP-AuNPs in 10
551 mM $CaCl_2$ was prepared by ultracentrifugation on a bare mica substrate. All number
552 concentrations represent average and standard deviation of two independent replicates.
553

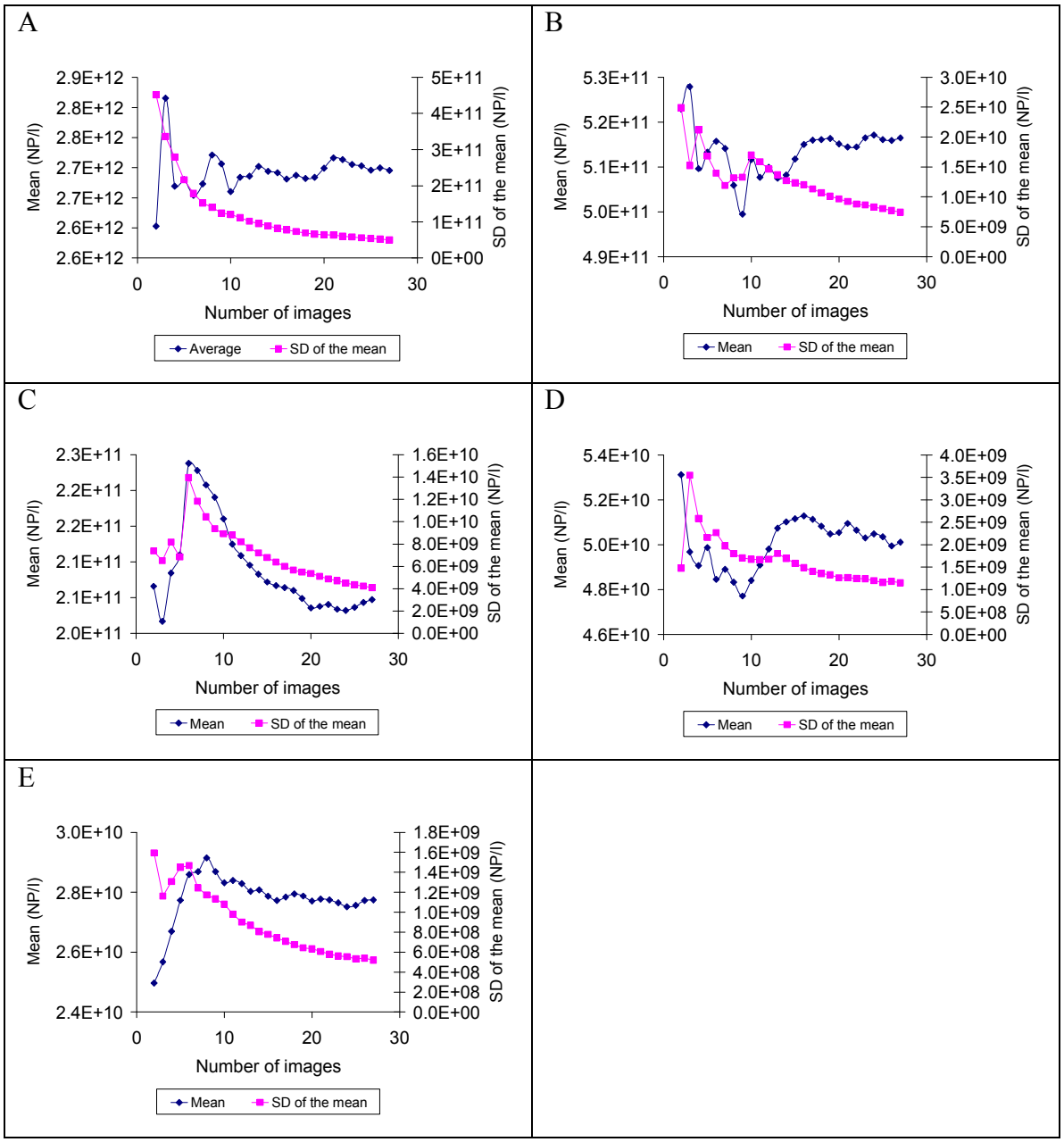

554

555 **Figure 3**. Dependence of the calculated mean number concentration and standard
556 deviation of the mean on the number of images scanned by atomic force microscopy of
557 the cit-AuNPs prepared by ultracentrifugation at 150 000 g on poly-l-lysine
558 functionalized AFM substrates at different concentrations (ppb): (a) 101.6, (b) 20.3, (c)
559 10.2, (d) 2.0 and (e) 1.0.

560

561

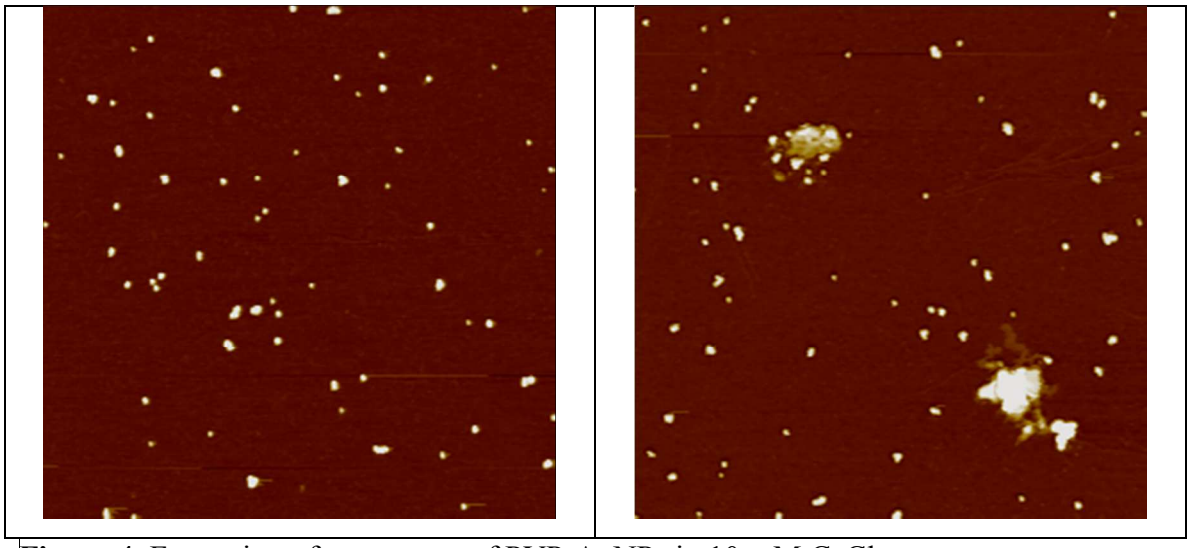

562 **Figure 4**. Formation of aggregates of PVP-AuNPs in 10 mM $CaCl_2$
563
564

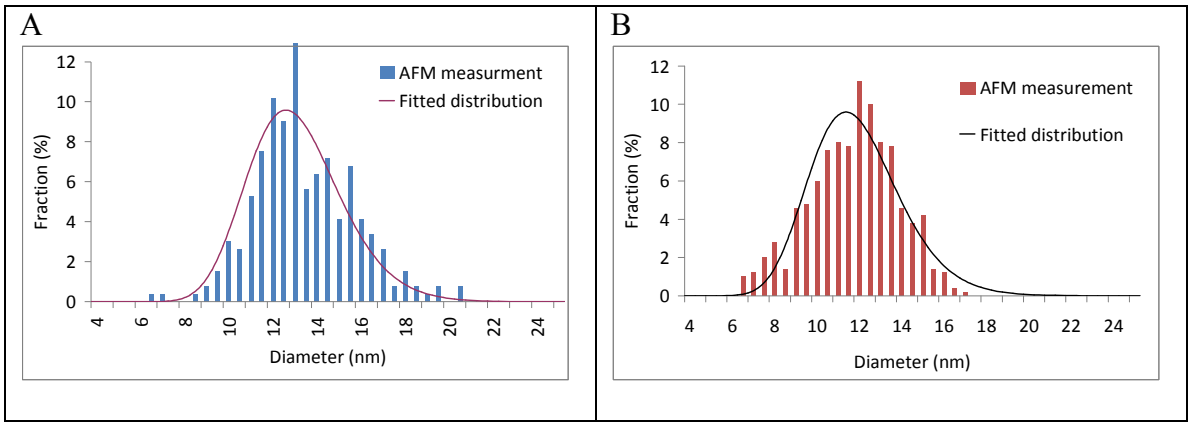

Figure 5. Particle size distribution as measured by atomic force microscopy and best log-normal fit of the AFM distribution of (A) Cit-AuNPs (13.3±2.1) suspended in UHPW and ultracentrifuged on poly-l-lysine functionalized mica substrate and (B) PVP-AuNPs (12.2±2.2) suspended in 10 mM $CaCl_2$ and ultracentrifuged on freshly cleaved bared mica substrate.

570 **Table 1**: Number concentration (particle.L^{-1}) of Cit-AuNPs in stock solutions

Concentration (ppb)	UHPW-B1 CV	UHPW-B2 CV	100 µM $CaCl_2$ CV	200 µM $CaCl_2$ CV	300 µM $CaCl_2$ CV	Poly-l-lysine B1 CV	Poly-l-lysine B2 CV
203.2	NA	NA	1.48×10^{13} 0.42	2.04×10^{14} 0.06	1.19×10^{14} 0.73	OL	OL
101.6	6.22×10^{12} 0.22	8.13×10^{12} 0.46	ND	2.84×10^{14} 0.16	5.29×10^{13} 0.73	2.70×10^{15} 0.10	2.67×10^{15} 0.10
20.3	NC	NA	8.77×10^{13} 0.24	2.50×10^{14} 0.34	6.36×10^{14} 0.26	2.58×10^{15} 0.07	2.54×10^{15} 0.08
10.2	NA	NA	ND	3.12×10^{14} 0.27	8.96×10^{13} 0.28	2.05×10^{15} 0.10	2.02×10^{15} 0.06
2.0	NA	NA	9.96×10^{14} 0.24	8.64×10^{14} 0.27	4.39×10^{14} 0.93	2.53×10^{15} 0.12	2.10×10^{15} 0.18
1.0	NA	NA	ND	1.04×10^{15} 0.34	1.13×10^{15} 0.17	2.77×10^{15} 0.10	2.17×10^{15} 0.12

571 NA: Not analysed
572 ND: not detected/not sufficient number of NPs to be counted
573 OL: overloading
574 WA: waiting analysis
575 UHPW: ultrahigh purity water
576

577 **Table 2**: Number concentration (particle.L^{-1}) of PVP-AuNPs in stock solutions

Concentration (ppb)	UHPW-Batch1 CV	UHPW-Batch2 CV	UHPW-Batch3 CV	10 mM $CaCl_2$-Batch1 CV	10 mM $CaCl_2$-Batch2 CV
670.5, 335.3 and 167.6	Overloading	NA	NA	NA	NA
67.1	ND	4.41×10^{15} 0.05	2.77×10^{15} 0.63	2.78×10^{15} 0.14	3.40×10^{15} 0.08
33.5	1.29×10^{15} 0.25	4.72×10^{14} 0.26	ND	3.38×10^{15} 0.09	2.07×10^{15} 0.17
16.8	NA	ND	ND	2.17×10^{15} 0.13	2.10×10^{15} 0.09
3.4	NA	ND	ND	3.11×10^{15} 0.15	2.58×10^{15} 0.10
1.7	NA	ND	ND	2.51×10^{15} 0.14	2.73×10^{15} 0.11
0.34	NA	ND	ND	3.79×10^{15} 0.33	3.72×10^{15} 0.24

578 NA: Not analysed
579 ND: not detected/not sufficient number of NPs to be counted
580 CV: coefficient of variation
581 UHPW: ultrahigh purity water
582
583

584 **Table 3.** Recovery (%) of Cit- and PVP-AuNPs by ignoring and considering size
585 polydispersity. The Cit-AuNPs prepared by Ultracentrifugation on a mica substrate
586 functionalized by poly-l-lysine. The PVP-AuNPs were prepared by ultracentrifugation on
587 a bare mica substrate from 10 mM $CaCl_2$ suspension.
588

Concentration of Cit-AuNPs (ppb)	Poly-l-lysine B1[a]	Poly-l-lysine B1[b]	Concentration of PVP-AuNPs (ppb)	10 mM $CaCl_2$-B1[a]	10 mM $CaCl_2$-B1[b]
101.6	63.8	70.9	67.1	30.2	33.2
20.3	61.1	64.1	33.5	36.7	40.3
10.2	48.5	52.3	16.8	23.7	26.0
2.0	59.3	66.0	3.4	33.8	37.1
1.0	65.7	68.9	1.7	27.3	30.0
			0.34	41.2	45.3

589 a: Ignoring polydispersity
590 b: Considering polydispersity
591